# Potential reduction interior point algorithm unfolding of neutron energy spectrum measured by recoil proton method *

Guan-Ying Wang(王冠鹰)[1] Ran Han(韩然)[1,2;1)] Xiao-Ping Ouyang(欧阳晓平)[1,3]
Jin-Cheng He(何锦成)[1] Jun-Yao Yan(颜俊尧)[1]

[1] North China Electric Power University, Beijing 102206, China
[2] Beijing Institute of Spacecraft Environment Engineering, Beijing 100029, China
[3] Northwest Institute of Nuclear Technology, Xi'an 710024, China

**Abstract:** A reconstruction algorithm for unfolding neutron energy spectra has been developed, based for the first time on the potential reduction interior point algorithm. This algorithm can be easily applied to neutron energy spectrum reconstruction in the recoil proton method. We transform the neutron energy spectrum unfolding problem into a typical nonnegative linear complementarity problem. The recoil proton energy spectrum and response matrix at angles of 0° and 30° are generated by the Geant4 simulation toolkit. Several different neutron energy test spectra are also employed. It is found that this unfolding algorithm is stable and provides efficient, accurate results.

**Keywords:** neutron energy spectrum, recoil proton, Geant4, potential reduction interior point algorithm, unfolding

**PACS:** 29.25.Dz, 29.30.Ep, 29.30.Hs **DOI:** 10.1088/1674-1137/41/5/056201

## 1 Introduction

The neutron energy spectrum is of great significance in both experimental research and theoretical analysis. It carries a large amount of information about the characteristics of the nuclear reaction system [1]. Recoil proton detectors (e.g. those based on liquid scintillators and Si(Au) surface barrier detectors) are often used to measure the neutron energy spectrum [2–4]. The recoil proton method is a common method for measuring the neutron energy spectrum. It is widely used for high resolution measurement in cases with low intensity and wide pulse width radiation field, where other methods have difficulty [5].

For neutrons incident on a polyethylene target after collimation, elastic scattering occurs between the hydrogen nuclei in the polyethylene film and the neutrons [6]. Some of the recoil protons enter into a detector which is set at a certain angle. The detector directly records the recoil proton energy spectrum. The process of unfolding is to obtain the real neutron energy spectrum through the recoil proton energy spectrum and the response function.

To unfold the neutron energy spectrum, several mathematical methods and computing codes have been developed, such as maximum entropy deconvolution [7], genetic algorithms [8], GRAVEL code [9], and populated artificial neural networks (ANNs) [10, 11]. GRAVEL is developed by the PTB Laboratory. It is widely used in the field of energy spectrum unfolding. Maximum entropy deconvolution, genetic algorithms and ANNs have been developed and applied to unfolding the neutron energy spectrum in recent years. In summary, these methods are all able to unfold neutron energy spectra. However, the accuracy and efficiency of these methods is not as good as expected. Therefore, finding a stable method to unfold the neutron energy spectrum is urgently required.

The purpose of this paper is to present a method to unfold the neutron energy spectrum based on the potential reduction interior point algorithm. In addition, other types of neutron energy test spectra are also employed. The resulting solutions show the good behavior of this algorithm. It is sufficiently fast, accurate, and robust for measurement of the neutron energy spectrum.

## 2 Principle of neutron energy spectrum unfolding

The recoil proton response $P(E')$ of a detector to a neutron energy spectrum $N(E)$ can be written as a first kind Fredholm integral function:

Received 09 December 2016
* supported by Fundamental Research Funds for Central Universities (2016XS61), and Opening Foundation of State Key Laboratory of Intense Pulsed Radiation Simulation and Effect.
1) E-mail: hanran@ncepu.edu.cn

$$P(E')=\int_{E_{\min}}^{E_{\max}} R(E,E')N(E)\,\mathrm{d}E, \tag{1}$$

where $P(E')$ denotes the recoil proton energy spectrum, $N(E)$ denotes the neutron energy spectrum, and $R(E,E')$ is the detector response. The basic task of neutron energy spectrum unfolding is to determine $N(E)$ from the measured recoil proton energy spectrum $P(E')$ according to the detector response $R(E,E')$. This is a typical inverse problem which $R(E,E')$ and $P(E')$ are known and $N(E)$ is unknown.

If we break $E$ and $E'$ into discrete intervals, then the integral Eq. (1) is rewritten as a discrete matrix as follows:

$$P_i=\sum R_{ij}N_j, \tag{2}$$

where $N_j$ represents the neutron energy spectrum in discrete form, and $j$ is the energy group number. $P_j$ is similar. It represents the recoil proton energy spectrum in discrete form, where $i$ is the energy group number. When the energy group number $i,j$ is large enough, Eq. (2) can replace Eq. (1).

In general, unfolding the neutron energy spectrum is very difficult. The response of the detector $R_{i,j}$ is usually ill conditioned, so minute perturbations can cause large fluctuations in the solution result. In addition, the first kind Fredholm integral function is a typical ill-posed problem – a solution may not exist, or exists but is not unique or depends on the initial conditions. Therefore, how to accurately solve the ill conditioned Eq. (2) is the key problem in the study of neutron energy spectrum unfolding.

## 3 Potential reduction interior point algorithm

The interior point algorithm was first proposed to solve linear programming problems by Karmarkar in 1984 [12]. Up to the present day, it has been a very active direction in the field of linear programming. The potential reduction interior point algorithm is developed from the interior point algorithm. In this paper, we for the first time apply this algorithm to unfold the neutron energy spectrum.

This algorithm is derived from Ref. [13]. Firstly, we transform the inverse problem in Eq. (2) into a least squares problem. Consider a typical least squares equation:

$$\min_{x\in R} f(x)=\|Ax-b\|^2, \tag{3}$$

where $A\in R^{m\times n}(m\geqslant n), b\in R^m, x\in R^n$.

The necessary and sufficient conditions to achieve the optimal solution can be summarized as follows:

$$\begin{cases} x^{\mathrm{T}}(A^{\mathrm{T}}Ax-A^{\mathrm{T}}b)=0 \\ A^{\mathrm{T}}Ax-A^{\mathrm{T}}b\geqslant 0 \\ x\geqslant 0. \end{cases} \tag{4}$$

Assume that $M=A^{\mathrm{T}}A, q=-A^{\mathrm{T}}b$, where $M$ is a positive semidefinite matrix. Then the above conditions can be transformed into a monotonic linear complementarity problem (LCP $(M,q)$):

$$\begin{cases} x^{\mathrm{T}}y=0 \\ y=Mx+q \\ x\geqslant 0, \quad y\geqslant 0. \end{cases} \tag{5}$$

Then, the potential function is constructed:

$$\Phi(x,y)=(n+\rho)\log\left(x^{\mathrm{T}}y\right)-\sum_{i=1}^{n}\log(x_iy_i)-n\log(n), \tag{6}$$

where $\rho$ is an iterative parameter and $n$ is the matrix order.

Note that $S_{++}=\{(x,y):y=Mx+q, x>0, y>0\}$ is the strictly feasible interior point for LCP $(M,q)$.

The basic concept of the potential reduction interior point algorithm is to adjust the iteration step that satisfies the solution of the linear complementarity problem, while at the same time, the potential function value is decreased.

$$\begin{cases} (x+\theta\Delta x, y+\theta\Delta y)\in S_{++} \\ \Phi(x+\theta\Delta x, y+\theta\Delta y)-\Phi(x,y)\leqslant -\delta, \end{cases} \tag{7}$$

where $\delta$ is a parameter.

The iteration direction $(\Delta x,\Delta y)$ depends on the solution of the Newton direction and central path direction simultaneous equation group:

$$\begin{cases} y\Delta x+x\Delta y=h \\ -M\Delta x+\Delta y=0, \end{cases} \tag{8}$$

where $h=-\left[xy-\beta\dfrac{x^{\mathrm{T}}y}{n}e\right]$, and $\beta=\dfrac{n}{n+\rho}$. The new iteration direction can reach a satisfactory solution with high convergence speed. The termination condition is $(x^k)^{\mathrm{T}}y\leqslant\varepsilon$. Finally, the optimal solution is $x^k$.

According to theoretical derivation, when the parameter of the potential function $\rho=O(\sqrt{n})$, the solution of $(x^k,y^k)$ can be obtained after at most $O\left(\sqrt{n}\log\left(\varepsilon^{-1}2^{\Phi(x_0,y_0)/\rho}\right)\right)$ iterations.

## 4 Simulation and testing

In the response matrix, each row corresponds to a given neutron energy and each column corresponds to

a given pulse height. To unfold the measured neutron energy spectrum, it is required to precisely know the response function $R(E,E')$ of the detector for each particle energy $E$. The response matrix can be obtained by Monte Carlo simulation.

Geant4 is a package developed by CERN to simulate the performance of detectors in nuclear and high energy physics [14]. The response matrix $R(E,E')$ of the mono-energetic neutrons in the polyethylene film should be confirmed according to the above iteration algorithm.

To test and verify this algorithm, the detection system geometry and its physical process are constructed in the Geant4 toolkit. The polyethylene target radius is 5 mm, its thickness is 18.4 mg/cm$^2$, the neutron source distance is 15 mm, and the energy from 1 MeV to 16 MeV in intervals of 0.1 MeV. On the other side of the polyethylene target, recoil protons are detected at angles of 0° and 30°. The geometry of the whole detection system is shown in Fig. 1. The recoil proton energy spectrum is then measured in discrete steps from 0.1 MeV to 16 MeV at intervals of 0.1 MeV. Thus, the recoil proton energy spectrum response matrices at 0° and 30° are obtained. We study the unfolding in different directions for two reasons. Firstly, the results can verify each other. Secondly, there will be different measurement directions in practice.

The potential reduction interior point algorithm was coded in MATLAB. The response matrix and recoil proton energy spectrum are brought into the program, and then we get the resulting solutions. Several neutron energy spectra with mono-energetic, multi-peak, Gaussian and double Gaussian distributions were used as output data to test the unfolding capability.

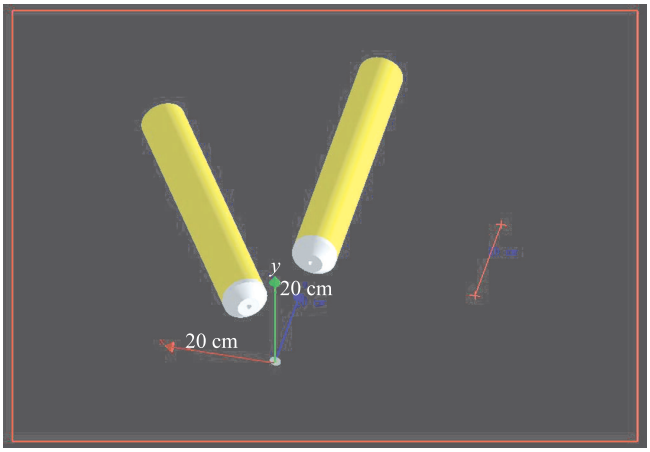


Fig. 1. (color online) Geometry of the whole detection system. The recoil proton detectors are placed at 0° and 30°.

## 5 Results and discussion

Figures 2–5 show the results of the unfolded energy spectrum. Figure 2 shows the results for a Gaussian neutron energy spectrum with $\sigma$=0.2 MeV, $\mu$=11.0 MeV. Figure 3 shows the results of a neutron energy spectrum with 4 peaks at 5, 7, 9 and 11 MeV, of which the intensity ratio is 1:2:3:4. Figure 4 shows the results of a double Gaussian neutron energy spectrum with $\sigma_1$=0.15 MeV, $\mu_1$=9.0 MeV, $\sigma_2$=0.15 MeV, $\mu_2$=13.0 MeV. Figure 5 shows the results of a neutron energy spectrum with 1 peak at 9.81 MeV.

We define $Q$ to evaluate the unfolded solution results [7]:

$$Q=\left[\frac{\sum_{i=1}^{n}\left(N_{i,\mathrm{Solution}}-N_{i,\mathrm{True}}\right)^2}{\sum_{i=1}^{n}\left(N_{i,\mathrm{True}}\right)^2}\right]^{\frac{1}{2}}. \tag{9}$$

Obviously, a perfect unfolded result would match the true spectrum exactly and give $Q=0$. The $Q$ values are listed in Table 1.

As can be seen from Figs. 2–5 and Table 1, whatever type of energy spectrum, the approximate results can be obtained in each direction, and the results at 0° are more accurate. The $Q$ values in that direction are smaller than the 30° results. The results at 30° show about 10% fluctuation compared with the true. The results in the low energy region are slightly inaccurate. The recoil proton energy spectra at 0° and 30° are received by the detector at the same time. However, as shown in Fig. 6, the outgoing direction of the recoil protons is concentrated in the forward direction. This will cause the recoil proton count in the direction of 30° to be less than 0°. In practice, if the intensity of the neutron source is low, we recommend that the detector be set close to 0°, so that it can receive more recoil protons. If the intensity of the neutron source is high, the detector should be set in other directions to avoid direct neutron irradiation. Overall, the results of 0° and 30° are reliable, and this algorithm can be applied to the neutron energy spectrum unfolding, but the results at 30° are not as accurate as at 0°.

Table 1. Evaluation of unfolded results for spectra in Figs. 2–5. $Q$ is defined in Eq. (9).

| | figure 2 Gaussian | figure 3 multi-peak | figure 4 double Gaussian | figure 5 mono-energetic |
|---|---|---|---|---|
| $Q$(0°) | 0.2304 | 0.0562 | 0.1041 | 0.0235 |
| $Q$(30°) | 0.3253 | 0.3090 | 0.3475 | 0.3097 |

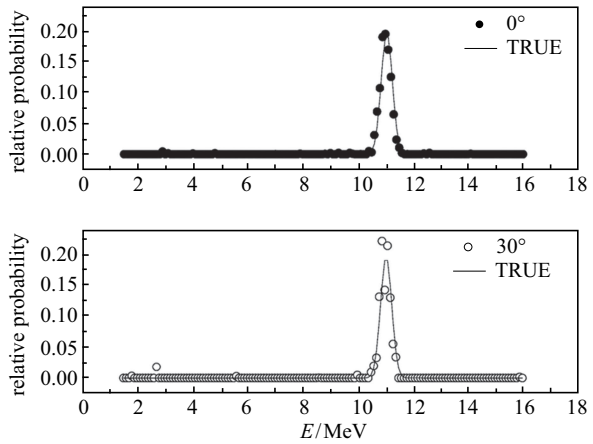


Fig. 2. Gaussian neutron energy spectrum with $\sigma$=0.2 MeV, $\mu$=11.0 MeV. The solid points represent the 0° results, the open circles represent the 30° results, and the solid line is the true neutron energy spectrum.

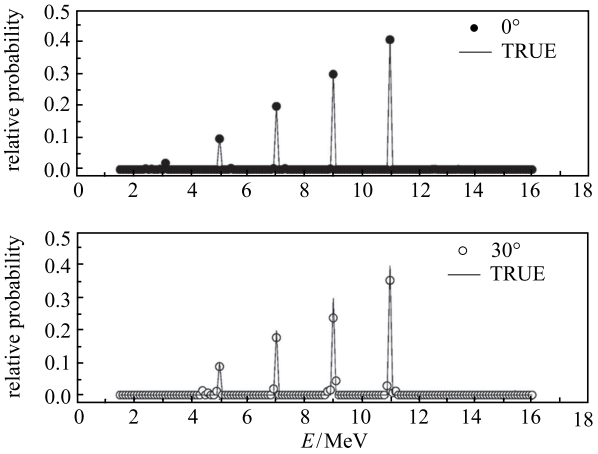


Fig. 3. Neutron energy spectrum with 4 peaks at 5, 7, 9 and 11 MeV, of which intensity ratio is 1:2:3:4. The solid points represent the 0° results, the open circles represent the 30° results, and the solid line is the true neutron energy spectrum.

The significant advantage of this algorithm is its speed of convergence to the optimal solution. It has a relatively high efficiency, compared with the general algorithms such as GRAVEL. Take the results of the Gaussian neutron energy spectrum in Fig. 2 as an example. To achieve the same accuracy with all other conditions identical, the GRAVEL algorithm takes 26794 steps while the potential reduction interior point algorithm takes only 13238 steps. The unfolding efficiency is increased by a factor of about 2.

As shown in Fig. 4 and Fig. 5, in the results at 30°, some outliers from the true solution are observed at low energy range (from 2 to 4 MeV). This is not obvious in the results at 0°, which show only tiny oscillations near the true energy spectrum range. There are two error sources. One is inaccurate results in the unfolding process caused by the algorithm, and is inevitable. The other is caused by the response matrix, and is mainly statistical error. The error in the 0° results is mainly the former and the error in the 30° results is mainly the latter.

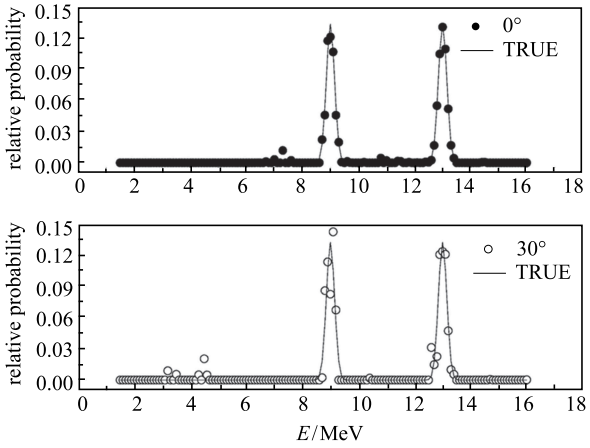


Fig. 4. Double Gaussian neutron energy spectrum with $\sigma_1$=0.15 MeV, $\mu_1$=9.0 MeV, $\sigma_2$=0.15 MeV, $\mu_2$=13.0 MeV. The solid points represent the 0° results, the open circles represent the 30° results, and the solid line is the true neutron energy spectrum.

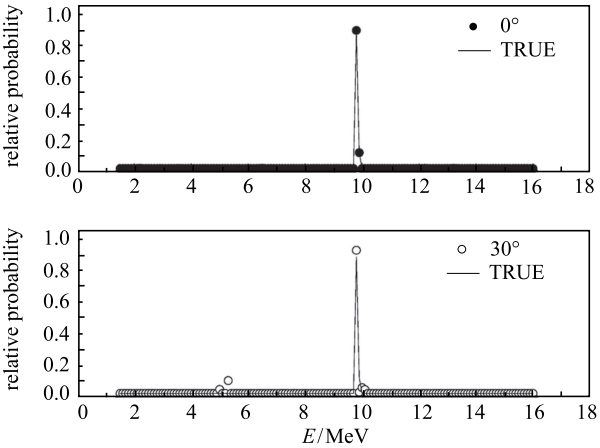


Fig. 5. Neutron energy spectrum with 1 peak at 9.81 MeV. The solid points represent the 0° results, the open circles represent the 30° results, and the solid line is the true neutron energy spectrum.

As an application example, Fig. 7 shows the D-T fusion neutron energy spectrum. This work can provide support for fusion neutron energy spectrum diagnosis. The data are from Ref. [15]. The full width at half maximum (FWHM) of the result and that of the true D-T fusion neutron energy spectrum is 1.1225 MeV and 1.1957 MeV respectively.

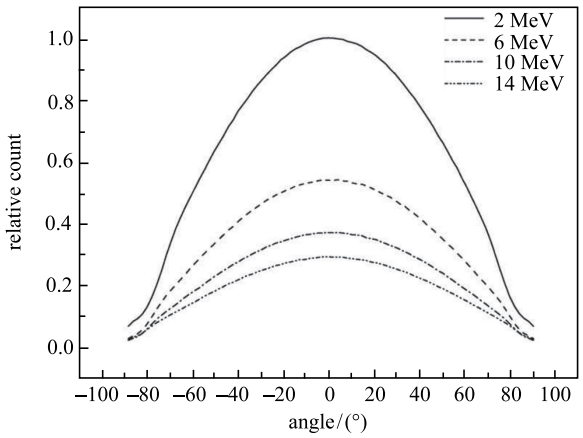


Fig. 6. Angular distribution of recoil proton at the moment when it is just generated, for different incident neutron energies.

In sum, the potential reduction interior point algorithm is stable and can obtain accurate solutions with fast convergence speed. The main purpose of this research is to confirm the ability of the unfolding algorithm, and the energy resolution of the detector is not considered.

## 6 Conclusion

In this paper, an algorithm based on the potential reduction interior point has been developed and applied to neutron spectrum unfolding for the first time. This algorithm selects the appropriate step length in each iteration process so that the value of the potential function decreases, and the iteration direction is the simultaneous solution of the central path direction and the Newton direction. It can be concluded that this algorithm is sufficiently fast and the solution results match the expected results. Additionally, results for a detector set at 0° are better than for a detector set at 30°. This indicates that the algorithm is sensitive to the response matrix. An application example for D-T fusion neutron energy spectrum unfolding was also shown.

Further work will focus on how to get more accurate results by using multiple direction data, and a new method called the multi-directional detection scheme will be discussed.

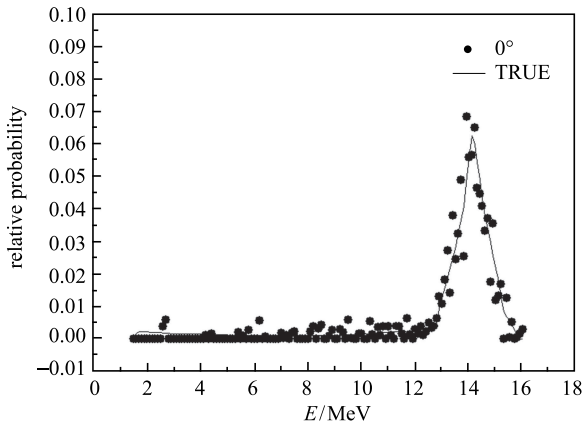


Fig. 7. D-T fusion neutron energy spectrum corresponding to the detector at 0°. The true data are taken from Ref. [15]. The solid points represent the 0° results, and the solid line is the true D-T fusion neutron energy spectrum.

## References


1 D. Z. Ding, C. T. Ye, Z. X. Zhao, *Neutron physics*, (Beijing: Atomic Energy Press, 2005), p. 10–50(in Chinese)
2 S. L. Wang, H. X. Huang, X. C. Ruan et al, Chin. Phys. C, **33**(5): 378–382 (2009)
3 L. An, Y. Chen, H. P. Guo et al, At. Energ. Sci.& Technol., **38**(s1-2): 89–92 (2004)(in Chinese)
4 H. P. Guo, L. An, X. H. Wang et al, At. Energ. Sci.& Technol., **41**(3): 283–287 (2007) (in Chinese)
5 J. L. Liu,*Study on an optical method for charged particle energy spectrum measurement*, Ph.D Thesis(Beijing:Tsinghua University, 2013)(in Chinese)
6 X. P. Ouyang, Eng. Sci., **11**(5): 44-53 (2009) (in Chinese)
7 M. Reginatto, P. Goldhagen, S. Neumann, Nucl. Instrum. Methods A, **476**(s1-2): 242–246 (2002)
8 D. W. Freeman, D. R. Edwards, A. E. Bolon, Nucl. Instrum. Methods A, **425**(3): 549–576 (1999)
9 M. Matzke, Unfolding of particle spectra, (1997)
10 A. Senada, A. Sara, P. Vladimir, Nucl. Instrum. Methods A, **565**(2): 742–752 (2006)
11 H R. Vega-Carrillo, E. Manzanares-Acua, GAM. Sanchez et al, Radia. Meas., **41**(4): 425–431 (2006)
12 N. Karmarkar, Combinatorica, **4**(4): 373–395 (1984)
13 S. Mizuno, F. Jarre, J. Stoer, Appl. Math. Opt., **33**(3): 315–341 (1996)
14 S. Agostinelli, J. Allison, K. Amako et al, Nucl. Instrum. Methods A, **506**(3): 250–303 (2003)
15 J. A. Frenje, R. Bionta, E. J. Bond et al, Nucl. Fusion, **53**(4): 043014 (2013)